

## VI-G Extreme UV Photoionization Studies of Fullerenes by Using a Grazing-Incidence Monochromator and High-Temperature Mass Spectrometer

On the beam line BL2B in UVSOR a grazing incidence monochromator has been constructed which supplies photons in the energy region from 20 to 200 eV [M. Ono, H. Yoshida, H. Hattori and K. Mitsuke, *Nucl. Instrum. Methods Phys. Res., Sect. A* **467-468**, 577–580 (2001)]. This monochromator was assumed to bridge the energy gap between the beam lines BL3B and BL4B, thus providing for an accelerating demand for the high-resolution and high-flux photon beam from the research fields of photoexcitation of inner-valence electrons, *L*-shell electrons in the third-row atom, and *4d* electrons of the lanthanides.

Since 2001 we have tried taking photoion yield curves of fullerenes. Geometrical structures and electronic properties of fullerenes have attracted widespread attention because of their novel structures, novel reactivity, and novel catalytic behaviors as typical nanometer-size materials. Moreover, it has been emphasized that the potential for the development of fullerenes to superconductors ( $T_c \sim 50$  K) and strong ferromagnetic substances is extremely high. In spite of such important species spectroscopic information is very limited in the extreme UV region, which has been probably due to difficulties in obtaining enough amount of sample. The situation has rapidly changed in these few years, since the techniques of syntheses, isolation, and purification have been advanced so rapidly that appreciable amount of fullerenes is obtainable from several distributors in Japan.

### VI-G-1 Refinements of the Estimation of Photoabsorption Cross Sections of Metallofullerenes

**KATAYANAGI, Hideki; PRODHAN, Md. Serajul Islam<sup>1</sup>; MITSUKE, Koichiro**  
(<sup>1</sup>SOKENDAI)

We have revisited the photoabsorption cross sections of endohedral metallofullerenes (Ce@C<sub>82</sub>, Dy@C<sub>82</sub> and Pr@C<sub>82</sub>) in the extreme ultraviolet<sup>1-3</sup>) and refined the procedure of their precise estimation. In the previous studies the cross sections were evaluated by comparing normalized count rates for the metallofullerenes with those for a standard sample. The cross sections thus obtained are found to serve as only crude approximations, since no consideration was given to the detection efficiency dependence of the time-of-flight mass spectrometer on sample masses and charges.

In the present study, we adopted an alternative approach to obtain more precise cross sections of the metallofullerenes. First, multiple standard samples having different masses were utilized for correction of the detection efficiency dependence. Second, such corrections were made by applying an empirical formula proposed by Twerenbold *et al.*<sup>4</sup>) Table 1 summarizes refined partial photofragmentation cross sections of Pr@C<sub>82</sub> and its total photoabsorption cross sections. All these values are the means of the two cross sections that were calculated using xenon and C<sub>60</sub> as standard samples. The deviations of the values in Table 1 are at most 12%, which implies that the detection efficiency dependence is fairly corrected. Indeed, the total photoabsorption cross section of 36 Mb at 110 eV is in good agreement with that of 82 carbon atoms, 33.5 Mb. Refinements of the cross sections of other metallofullerenes using several standard samples are also in progress.

#### References

1) K. Mitsuke, T. Mori, J. Kou, Y. Haruyama and Y. Kubozono, *J. Chem. Phys.* **122**, 064304 (2005).

- 2) K. Mitsuke, T. Mori, J. Kou, Y. Haruyama, Y. Takabayashi and Y. Kubozono, *Int. J. Mass Spectrom.* **243**, 121 (2005).  
3) H. Katayanagi, B. P. Kafle, J. Kou, T. Mori, K. Mitsuke, Y. Takabayashi, E. Kuwahara and Y. Kubozono, *J. Chem. Phys.* submitted.  
4) D. Twerenbold, D. Gerber, D. Gritti, Y. Gonin, A. Netuschil, F. Rossel, D. Schenker and J. L. Vuilleumier, *Proteomics* **1**, 66 (2001).

**Table 1.** Partial photofragmentation cross sections of Pr@C<sub>82</sub> for the formation of Pr@C<sub>82</sub><sup>z+</sup> and the total photoabsorption cross sections at the photon energies of 110 and 130 eV. All cross sections are in Mb.

Photon energy	Photofragmentation cross section		Total cross section
	Pr@C <sub>82</sub> <sup>+</sup>	Pr@C <sub>82</sub> <sup>2+</sup>	
110 eV (off-resonance)	22.2	13.8	36.0
130 eV (on-resonance)	32.7	22.6	55.3

### VI-G-2 Fragmentation Mechanism of Highly Excited C<sub>70</sub> Cations in the Extreme Ultraviolet

**MITSUKE, Koichiro; KATAYANAGI, Hideki; KOU, Junkei; MORI, Takanori; KUBOZONO, Yoshihiro<sup>1</sup>**  
(<sup>1</sup>Okayama Univ.)

[*AIP Conf. Proc.* **811**, 161–166 (2006)]

The ion yield curves for C<sub>70-2n</sub><sup>z+</sup> ( $n = 1-8$ ,  $z = 2$  and 3) produced by photoionization of C<sub>70</sub> were measured in the photon energy ( $h\nu$ ) range of 25–150 eV. The appearance  $h\nu$  values were higher by *ca.* 34 eV than the thermochemical thresholds for dissociative ionization of C<sub>70</sub> leading to C<sub>70-2n</sub><sup>z+</sup> (see Figure 1). Evaluation was made on the upper limits of the internal energies of the primary C<sub>70</sub><sup>z+</sup> above which C<sub>70-2n+2</sub><sup>z+</sup> fragments cannot escape from further dissociating into C<sub>70-2n</sub><sup>z+</sup> + C<sub>2</sub>. These critical internal energies agreed well with appearance internal energies of C<sub>70</sub><sup>z+</sup> theoretically obtained

corresponding to the threshold for the formation of  $C_{70-2n}^{z+}$ . The photofragmentation of the parent  $C_{70}^{z+}$  ions is considered to be governed by the mechanism of internal conversion of their electronically excited states, statistical redistribution of the excess energy among a number of vibrational modes, and sequential ejection of the  $C_2$  units.

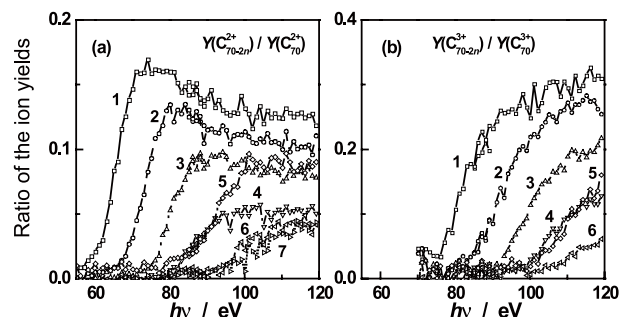


**Figure 1.** Relative ion yield curves of  $C_{70-2n}^{z+}$  ions obtained from time-of-flight mass spectra. (a)  $z = 2$ ,  $n = 1-7$  and (b)  $z = 3$ ,  $n = 1-6$ .

## VI-H Photoionization and Fragmentation Mechanisms of $C_{60}$ and $C_{70}$ in the Extreme Ultraviolet

When fullerenes gain enough amount of energy through photoionization processes, primarily formed ions are known to undergo decomposition into fragment ions with even numbered carbon atoms. We have measured the yield curves for  $C_{60-2n}^{z+}$  from  $C_{60}$  as a function of the internal energy  $E_{\text{int}}$  of the parent  $C_{60}^{z+}$  ions to study the mechanisms and kinetics of the above unimolecular reactions. These experimental yield curves have been compared with the theoretical fractional abundance curves. We found that the experimental and theoretical curves provide almost the same appearance internal energies for the formation of  $C_{60-2n}^{z+}$  ( $n \geq 1$ ). This result appears to reveal that the excess energy is statistically distributed among the internal degrees of freedom of the parent ions and that  $C_2$  units are ejected sequentially ( $C_{60}^{z+} \rightarrow C_{58}^{z+} + C_2$ ,  $C_{58}^{z+} \rightarrow C_{56}^{z+} + C_2$ , ...,  $C_{60-2n+2}^{z+} \rightarrow C_{60-2n}^{z+} + C_2$ ).

There remains ambiguity as to whether potential barrier exists along the reaction coordinate and whether resonant state participates during dissociation. Moreover, a few groups have argued that another mechanism of single-step two-fragment fission ( $C_{60}^{z+} \rightarrow C_{60-2n}^{z+} + C_{2n}$ ) could be involved in the formation of  $C_{60-2n}^{z+}$ . To elucidate these issues, we are developing two devices which are incorporated into the present photoionization spectrometer for gaseous fullerenes: photofragment imaging analyzer and threshold photoelectron-photoion coincidence apparatus.

### VI-H-1 Kinetic Energy Analysis of the Fragment Ions Produced from $C_{60}$ and $C_{70}$

**KATAYANAGI, Hideki; KAFLE, Bhim Prasad<sup>1</sup>;  
PRODHAN, Md. Serajul Islam<sup>1</sup>; YAGI, Hajime;  
MITSUKE, Koichiro  
(<sup>1</sup>SOKENDAI)**

We have reported the yield curves<sup>1,2)</sup> of the fragments  $C_{60-2n}^{z+}$  and  $C_{70-2n}^{z+}$  ( $n = 1$ ,  $z = 1$ ) produced by photoionization of solitary  $C_{60}$  and  $C_{70}$ , respectively, in the photon energy range of 45–150 eV. Then the mechanism of sequential loss of  $C_2$  units has been proposed on a basis of comparison between the experimental ion yield curves and theoretical fractional abundance curves. The latter curves have been derived by employing the RRKM theory to individual unimolecular reactions,  $C_{60-2n+2}^{z+} \rightarrow C_{60-2n}^{z+} + C_2$ . More reliable calculations of the rate constants of the consecutive reactions are needed before closer comparison between the two curves. For such calculations we should know precise values of the activation energies for the reactions, together with the vibrational spectra of the transition states. This induced us to develop a new ion spectrometer for the fragment ions produced from  $C_{60}^{z+}$  and

$C_{70}^{z+}$ . It is likely that the magnitude of the potential barriers of the reactions can be estimated from the average kinetic energy release measured by this spectrometer.

#### References

- 1) J. Kou, T. Mori, Y. Kubozono and K. Mitsuke, *Phys. Chem. Chem. Phys.* **7**, 119 (2005).
- 2) K. Mitsuke, H. Katayanagi, J. Kou, T. Mori and Y. Kubozono, *AIP Conf. Proc.* **811**, 161 (2006).

### VI-H-2 Photofragment Imaging Apparatus for Measuring Momentum Distributions in Dissociative Photoionization of Fullerenes

**KAFLE, Bhim Prasad<sup>1</sup>; PRODHAN, Md. Serajul Islam<sup>1</sup>; KATAYANAGI, Hideki; MITSUKE, Koichiro  
(<sup>1</sup>SOKENDAI)**

[AIP Conf. Proc. in press]

We are developing a photofragment imaging apparatus based on time-of-flight (TOF) mass spectrometry to measure the kinetic energy and angular distributions

of the fragments. We have adopted the Eppink–Parker type three-element velocity focusing lens system<sup>1)</sup> (electrodes R, E, and T) to achieve high kinetic energy resolution on the photofragment images. Furthermore, we have utilized a potential switchable mass gate M and an ion reflector G inside the TOF tube as demonstrated in Figure 1, to select a bunch of fragments having the same mass-to-charge ratio  $m/z$  from neighboring bunches  $(m \pm 24)/z$ . As long as M is kept grounded, all fragments are reflected back by G and do not impinge against the imaging detector PSD. When an entire bunch of the fragments having an expected  $m/z$  arrives inside M, a pulsed voltage is applied there. The potential energies of the ions in this bunch are suddenly elevated, so that these ions can exclusively pass through G and reach the PSD.

For optimizing the dimensions of the setup, we have performed ion trajectory simulations utilizing the SIMION software. We considered that the dissociative ionization of  $C_{60}$  takes place within a region of rectangular parallelepiped  $\Delta x \Delta y \Delta z = 1 \times 3 \times 1 \text{ mm}^3$  in the ionization region of the spectrometer. The simulated trajectories of  $C_{60}^+$ ,  $C_{58}^+$  and  $C_{56}^+$  at initial kinetic energy of 0.1 eV show that the trajectories of unwanted  $C_{60}^+$  and  $C_{56}^+$  ions are reflected completely. On the other hand, most of the trajectories of  $C_{58}^+$ , the ion whose momentum image we wish to measure, are found to go beyond G and reach the PSD. This observation provides direct evidence for exclusive imaging detection of  $C_{58}^+$ .

#### Reference

- 1) A. T. J. B. Eppink and D. H. Parker, *Rev. Sci. Instrum.* **68**, 3477 (1997).



**Figure 1.** Schematic view of the momentum imaging spectrometer and simulated trajectories of  $C_{58}^+$  at initial kinetic energies of 0.1 eV. R, repeller; E, extractor; T, entrance electrode of a time-of-flight drift tube (TOF); IT, Ion trajectories; M, mass gate; G, ion reflector. The dimensions of all the electrodes are determined from the SIMION 3D software.

#### VI-H-3 Simulated Image of Fragment Ions Produced from $C_{60}$

**KAFLE, Bhim Prasad<sup>1</sup>; PRODHAN, Md. Serajul Islam<sup>1</sup>; YAGI, Hajime; KATAYANAGI, Hideki; MITSUKE, Koichiro**  
(<sup>1</sup>SOKENDAI)

Our photofragment imaging spectrometer under construction is found to realize excellent momentum imaging detection of fullerene fragments with a particular cluster size. To demonstrate its capability, we have reproduced a simulated image of fragment ions  $C_{58}^+$  from  $C_{60}$  with different kinetic energies. Figure 1 shows the image of the  $C_{58}^+$  ions on the PSD at the kinetic energies of 0.1 eV (triangles) and 0.11 eV (circles). We have taken into account the ion trajectories generated in

the elevation and azimuth angle ranges of  $0^\circ$  to  $+90^\circ$  and  $0^\circ$  to  $+180^\circ$ , respectively, which cover only one quarter of the full three-dimensional trajectories over the  $4\pi$  solid angle. The trajectories with a given elevation angle form a horizontal stripe, and the envelope of all the stripes makes an arc. This clearly demonstrates that scattering distribution in spherical symmetry can be successfully projected on an image plane. It is likely that the two images are almost separable if their kinetic energy difference is larger than 0.01 eV. Comparison between the simulations with and without the ion reflector G (see Figure 1 of VI-H-2) confirmed that the images are not distorted in the presence of G. The present momentum imaging spectrometer will be installed at the end station of beam line 2B in the UVSOR facility.

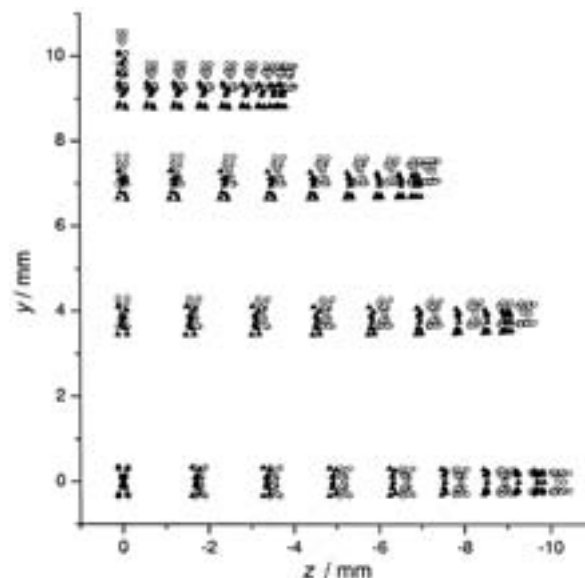


**Figure 1.** Simulated image of  $C_{58}^+$  ions at the kinetic energies of 0.1 eV (▲) and 0.11 eV (○). The three-dimensional scattering distribution of the ions is projected on the PSD.

#### VI-H-4 Scattering Distributions of the Photofragments from $C_{60}$ in the Extreme Ultraviolet

**PRODHAN, Md. Serajul Islam<sup>1</sup>; KAFLE, Bhim Prasad<sup>1</sup>; YAGI, Hajime; KATAYANAGI, Hideki; MITSUKE, Koichiro**  
(<sup>1</sup>SOKENDAI)

In thermodynamic equilibrium the velocity distribution of a large number of  $C_{60}$  molecules can be represented by the Maxwell-Boltzmann form of

$$f_0(\vec{v}) \propto \left[ \frac{m}{2\pi kT} \right]^{\frac{3}{2}} \exp\left( \frac{-mv^2}{2kT} \right) \quad (1)$$

where the density and temperature are assumed to be independent of the positions of molecules. Therefore, the velocity distribution of the photofragments from  $C_{60}$  in the laboratory system can be expressed as that in the center-of-mass system convoluted with the initial Maxwell-Boltzmann distribution before photoionization. We will perform deconvolution procedure to derive the

velocity distribution in the center-of-mass system, which is needed to decide on a dominant mechanism in fragmentation of electronically excited  $C_{60}$  cations, from the three-dimensional velocity distributions of the fragment ions measured by using our imaging spectrometer.

#### VI-H-5 Why We Wish to Measure the Yield Curves of the Photofragments from $C_{60}$ in Coincidence with Threshold Electrons

MITSUKE, Koichiro; KATAYANAGI, Hideki;  
KAFLE, Bhim Prasad<sup>1</sup>; PRODHAN, Md. Serajul  
Islam<sup>1</sup>; YAGI, Hajime  
(<sup>1</sup>SOKENDAI)

We have derived the  $E_{\text{int}}$ -dependence of the  $C_{60-2n}^{z+}$  yield from the experimental  $h\nu$ -dependent yield, and then compared the former dependence with the theoretical fractional abundance near the onset region.<sup>1)</sup> Such a comparison may become less meaningful further away from the onset region. This is because, in our estimate of  $E_{\text{int}}$  of the primary  $C_{60}^{z+}$ , we have disregarded the energy transmission from a portion of  $h\nu$  to the photoelectron kinetic energy, and eventually substantial errors have been produced in the  $E_{\text{int}}$ -dependence curve. To convert the  $h\nu$ -dependent yield accurately to the  $E_{\text{int}}$ -dependence, we require the partial photoionization cross section of  $C_{60}$  for the formation of  $C_{60}^{z+}$  as a function of both  $h\nu$  and  $E_{\text{int}}$ . However, it is far from easy to obtain the partial photoionization cross section in wide  $h\nu$  and  $E_{\text{int}}$  ranges from conventional two-dimensional photoelectron spectroscopy. Thus we are planning to measure (a) the yield curve of threshold electrons and (b) that of  $C_{60-2n}^{z+}$  in coincidence with the threshold electrons. Using these two curves we will be able to calculate a proper  $E_{\text{int}}$ -dependence of the  $C_{60-2n}^{z+}$  yield.

#### Reference

- 1) K. Mitsuke, H. Katayanagi, J. Kou, T. Mori and Y. Kubozono, *AIP Conf. Proc.* **811**, 161 (2006).

#### VI-H-6 ZEKE Photoelectron Spectroscopy Utilizing the Dark Gap of UVSOR Storage Ring

KATAYANAGI, Hideki; KAFLE, Bhim Prasad<sup>1</sup>;  
PRODHAN, Md. Serajul Islam<sup>1</sup>; YAGI, Hajime;  
MITSUKE, Koichiro  
(<sup>1</sup>SOKENDAI)

Last year we constructed a threshold photoelectron spectrometer for the purpose of measuring the signal of threshold electron-photoion coincidence (TEPICO), using the dark gap of the synchrotron radiation facility. Such measurements provide us with the detailed information about the excitation/dexcitation and decay processes of gaseous fullerenes ( $C_{60}$  and  $C_{70}$ ). We already succeeded in observing the threshold electron signal using He and  $O_2$  samples, but the spectra suffered from intense background counts. The background needs to be reduced to the utmost for performing the TEPICO measurement. Also an improvement of the spectrometer in the efficiency for threshold electrons is urgently needed. For these requirements, we are now developing an

improved version of the spectrometer which has the capability to significantly reject the electrons with high kinetic energies and to guide electrons with zero or very small kinetic energies (0 to 10 meV) to the detector.

#### VI-H-7 New Design of a ZEKE Photoelectron Spectrometer for Photofragmentation Studies of Fullerenes

KAFLE, Bhim Prasad<sup>1</sup>; KATAYANAGI, Hideki;  
MITSUKE, Koichiro  
(<sup>1</sup>SOKENDAI)

Figure 1 shows a schematic diagram of our improved threshold photoelectron spectrometer, together with typical trajectories for 10 meV photoelectrons. Here, a voltage of  $E_E = 3$  V is applied to the extraction electrode. The extraction and screening electrodes are 1 mm in thickness and central circular apertures of 7 mm in diameter are drilled. The arrangement of the electrodes was optimized by using the SIMION software.<sup>1)</sup> We have adopted penetrating field technique which was invented by King and coworkers.<sup>2)</sup> In this technique a potential well is formed in the ionization region by the field penetration from the potential of the extraction electrode through the screening electrode, providing a very large solid angle of collection for slow electrons ( $\sim 4\pi$  sr). Slow electrons are focused again at a crossover point inside a three-element asymmetric lens system beyond which they can reach the detector. In contrast, high energy electrons are strongly suppressed by the field of the asymmetric lens system. The proportion of the detectable trajectories is determined by simulation as a function of the electron kinetic energy. The results at  $E_E = 3$  V are shown in Figure 2.

#### References

- 1) D. A. Dahl, SIMION 3D Version 7.0 User's Manual, Idaho falls: 2000.
- 2) R. I. Hall, A. McConkey, K. Ellis, G. Dawber, L. Avaldi, M. A. MacDonald and G. C. King, *Meas. Sci. Technol.* **3**, 316 (1992).



**Figure 1.** Schematic view of the threshold photoelectron spectrometer and simulated trajectories at the initial kinetic energy of 10 meV. From ionization center 36 electron trajectories were generated in the ejection angle of  $0^\circ$  to  $360^\circ$ , at an interval of  $10^\circ$ . R, repeller; S, screening electrode; E, extraction electrode; A, asymmetric lens system; F, front-plate electrode.

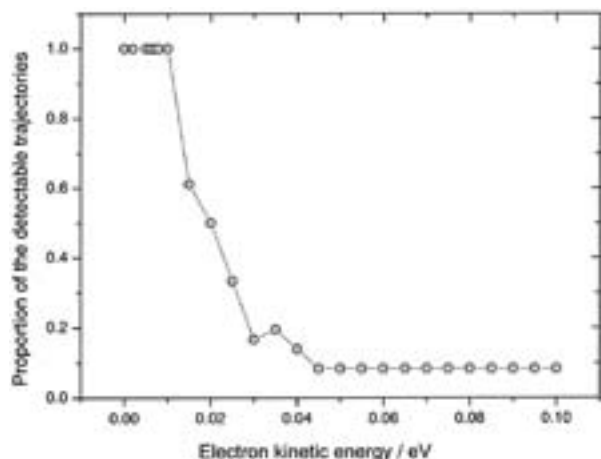


**Figure 2.** Proportion of the detectable trajectories determined by simulation at  $E_E = 3$  V. The curve shows a sharp increase below 20 meV.

### VI-H-8 High Resolution Photoelectron Spectroscopy of Gaseous Fullerenes

**YAGI, Hajime; KATAYANAGI, Hideki; KAFLE, Bhim Prasad<sup>1</sup>; PRODHAN, Md. Serajul Islam<sup>1</sup>; MITSUKE, Koichiro**  
(<sup>1</sup>SOKENDAI)

Photoemission measurements of solitary  $C_{60}$  and  $C_{70}$  have been made by several groups, but their energy resolution was *ca.* 100 meV at the best. We are developing an apparatus of high-resolution angle-resolved photoemission spectroscopy, using a helium discharge lamp or synchrotron radiation. Our goal is to carry out photoemission spectroscopy of various kinds of gaseous fullerenes with a total energy resolution of  $\sim 20$  meV. Fullerenes have a number of degenerated bands within 40 eV from the Fermi energy. Definite assignments of the peaks in the photoemission spectra of fullerenes are expected to be easier in the gas phase than in the solid phase, since band broadening and interference of secondary electrons are substantially reduced in the gas phase. Some of the peaks arising from excitations to different vibrational states of excited  $C_{60}^+$  ions might be distinguishable. As for metallofullerenes it is documented that electron transfer takes place from the encapsulated metal atoms to the fullerene cages. For instance, valence-band photoemission studies of the  $La@C_{82}$  film showed that new peaks due to triply electron transfer emerge near the Fermi energy. Such peaks are expected to be seen more clearly in the gas phase. By measuring the photoion yield curves, we observed for the first time the  $4d \rightarrow 4f$  giant dipole resonance in  $Ce@C_{82}$  and  $Pr@C_{82}$ . Using synchrotron radiation, we will perform resonant photoemission spectroscopy of these species to confirm the presence of giant dipole resonance and to study the dynamics of the  $4f$  electrons of encapsulated metal atoms.

### VI-H-9 Construction of an End Station of BL2B to Study Dissociative Photoionization of Fullerenes and VUV Spectroscopy of Ionic Liquids

**KATAYANAGI, Hideki; KAFLE, Bhim Prasad<sup>1</sup>; PRODHAN, Md. Serajul Islam<sup>1</sup>; YAGI, Hajime; MITSUKE, Koichiro**  
(<sup>1</sup>SOKENDAI)

A new vacuum chamber for the end station of beam line 2B (BL2B) in UVSOR was constructed. The chamber was designed for the gas phase spectroscopy of refractory materials such as fullerenes, metalloencapsulated fullerenes and ionic liquids. The following three subjects are now under way: (1) the velocity map imaging<sup>1)</sup> of the ionic photofragments from fullerenes, (2) threshold photoelectron-photoion coincidence measurements of the fullerenes, and (3) photoelectron and photoabsorption spectroscopy of ionic liquids. The installation of the chamber at BL2B was accomplished. We are going to instrument various spectrometers into the chamber for the above experiments.

Drawing of the chamber is shown in Figure 1. The twofold  $\mu$ -metal shield is put inside the chamber to prevent penetration of the geomagnetic field. The effective volume surrounded by the shield is five times as large as that of the previous chamber used at BL2B. The new chamber is equipped with 14 ports facing the ionization region, *i.e.* the focal point of the synchrotron radiation. This larger volume and versatile port arrangement enable us to incorporate many complicated devices. Moreover, we will use this chamber also at BL7U, a new beam line with a normal incidence monochromator connected with a planar undulator. Accordingly, the chamber was mounted on a micromotion stage in order to align its optical axis readily with the beam lines when the chamber is relocated.

#### Reference

- 1) A. T. J. B. Eppink and D. H. Parker, *Rev. Sci. Instrum.* **69**, 3477 (1997).

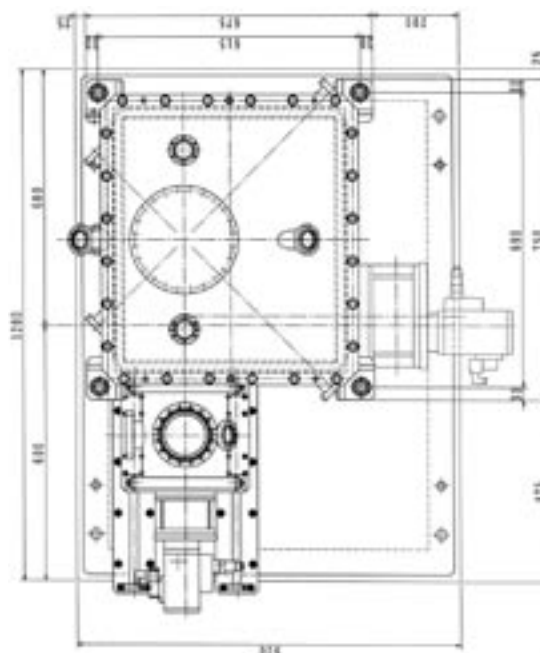


**Figure 1.** Drawing (top view) of the vacuum chamber on the micromotion stage (1200 × 900 mm) for the beam lines BL2B and BL7U in UVSOR.

## VI-I Ray-Tracing for the Branch Beam Line of the 10-m Normal Incidence Monochromator Developed for Gas-Phase Photochemistry

Domestic synchrotron radiation facilities have no undulator beam line devoted to studies on gas-phase photochemistry in the vacuum ultraviolet (VUV) region. Kimura and coworkers in the UVSOR facility are constructing a new undulator beam line BL7U equipped with normal incidence monochromator, aiming at a maximum flux of  $10^{11}$  photons/s (at 0.01% band width) and a maximum resolving power of 60000 [e.g. *UVSOR Activity Report* **2004**, 46 (2005)]. Our group is planning to construct a branch line to this monochromator. At the end station we will perform spectroscopic and dynamical studies of gas-phase molecules and clusters. Ray-tracing of the monochromator is in progress to determine the specifications of the branch line, with particular attention to the positions and shapes of post-focusing mirrors.

### VI-I-1 Layout of the Branch Beam Line of BL7U

MITSUKE, Koichiro

The detailed design of the beam line 7U has been reported elsewhere,<sup>1)</sup> so that we will briefly describe its layout (see Figure 1). The undulator is of APPLE-II type with a periodic length of 76 mm and the number of period of 38. Kimura and coworkers have adopted the normal incidence monochromator having an off-plane eagle mount in which three spherical gratings with 10-m focal length undergo translational and rotational motions. The undulator radiation is sampled by a pinhole, deflected horizontally at planar mirrors M0 and M1 by  $10^\circ$  and  $165^\circ$ , respectively, and made to irradiate the surface of one of the spherical gratings. The undulator radiation is further deflected horizontally at the grating by  $182^\circ$ . The dispersion plane of the grating lies vertically and the associated incidence and diffracted angles are always the same with varying from  $0^\circ$  ( $0^{\text{th}}$ -order light) to  $6^\circ$  (the longest wavelength). The  $1^{\text{st}}$ -order light of the grating is deflected horizontally at the planar steering mirror M2 by  $30^\circ$  and focused onto the exit slit in the horizontal and vertical directions simultaneously. The light is then deflected horizontally at the toroidal postfocusing mirror M4 by  $20^\circ$ , thereby focusing onto the ionization point in the end station.

### Reference

1) S. Kimura, *UVSOR Activity Report* **2004**, 46 (2005).

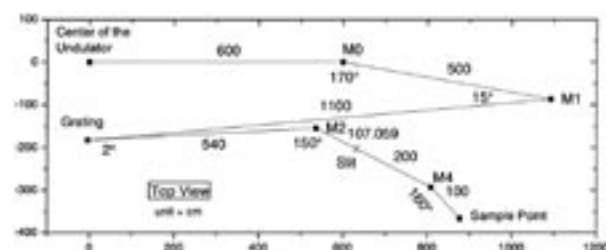


**Figure 1.** Layout of the beam line BL7U of UVSOR involving a 10-m normal incidence monochromator. The distances between two optical elements are in cm. Symbols  $M_n$  ( $0 \leq n \leq 4$ ) designate the pre- and post-focusing mirrors.

### VI-I-2 Ray-Tracing for the Branch Beam Line of BL7U of UVSOR

MITSUKE, Koichiro

The ray tracing is carried out at the fundamental of the undulator radiation around 17 eV at the deflection parameter of  $K = 2.5$  by making use of the Shadow software. Panels a and b of Figure 1 show the spot images at the exit slit and ionization point, respectively, when 20000 rays ranging in the photon energy from 17.0497 to 17.0500 eV are generated randomly. We employed a grating with 2400 lines/mm, a slit with a 20  $\mu\text{m}$ , and diffraction angle of  $5.00695^\circ$ . The sizes of the optical elements are taken into account, whereas their reflectivity and slope errors are neglected. The analysis showed that 6843 rays can arrive at the ionization point (Good rays) with a spot size of  $20 \mu\text{m} \times 400 \mu\text{m}$ . On the other hand, the number of the good rays is reduced to almost 3000, when the 20000 rays are generated in the photon energy range of either 17.0494–17.0497 eV or 17.0500–17.0503 eV. It is therefore likely that a resolving power of more than 30000 has been achieved. A resolving power of ca. 60000 is expected to be attained if we utilize a grating with 3600 lines/mm.

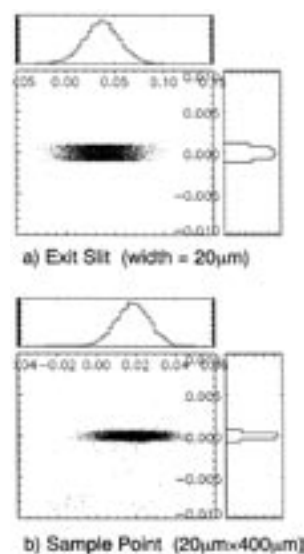


**Figure 1.** Spot images at the a) exit slit and b) ionization point under a 5%-coupling operation.